

Inter-annual variations of dissolved oxygen and hypoxia off the northern Changjiang River (Yangtze River) Estuary in summer from 1997 to 2014

Anqi Liu^{1, 2, 3}, Feng Zhou^{1, 2, 3*}, Xiao Ma^{2, 3*}, Qiang Zhao⁴, Guanghong Liao¹, Yuntao Zhou⁵, Di Tian^{2, 3}, Xiaobo Ni^{2, 3}, Ruibin Ding⁶

¹ College of Oceanography, Hohai University, Nanjing 210098, China

² State Key Laboratory of Satellite Ocean Environment Dynamics, Second Institute of Oceanography, Ministry of Natural Resources, Hangzhou 310012, China

³ Observation and Research Station of Changjiang River Delta Marine Ecosystems, Ministry of Natural Resources, Zhoushan 316022, China

⁴ Ningbo Marine Center, Ministry of Natural Resources, Ningbo 315000, China

⁵ School of Oceanography, Shanghai Jiao Tong University, Shanghai 200240, China

⁶ Institute of Polar and Ocean Technology, Second Institute of Oceanography, Ministry of Natural Resources, Hangzhou 310012, China

Received 28 March 2023; accepted 16 June 2023

© Chinese Society for Oceanography and Springer-Verlag GmbH Germany, part of Springer Nature 2024

Abstract

Hypoxia off the Changjiang River Estuary has been the subject of much attention, yet systematic observations have been lacking, resulting in a lack of knowledge regarding its long-term change and drivers. By revisiting the repeated surveys of dissolved oxygen (DO) and other relevant hydrographic parameters along the section from the Changjiang River Estuary to the Jeju-do in the summer from 1997 to 2014, rather different trends were revealed for the dual low-DO cores. The nearshore low-DO core, located close to the river mouth and relatively stable, shows that hypoxia has become more severe with the lowest DO descending at a rate of -0.07 mg/(L·a) and the thickness of low-DO zone rising at a rate of 0.43 m/a. The offshore core, centered around 40-m isobath but moving back and forth between 123.5° – 125° E, shows large fluctuations in the minimum DO concentration, with the thickness of low-DO zone falling at a rate of -1.55 m/a. The probable factors affecting the minimum DO concentration in the two regions also vary. In the nearshore region, the decreasing minimum DO is driven by the increase in both stratification and primary productivity, with the enhanced extension of the Changjiang River Diluted Water (CDW) strengthening stratification. In the offshore region, the fluctuating trend of the minimum DO concentration indicates that both DO loss and DO supplement are distinct. The DO loss is primarily attributed to bottom apparent oxygen utilization caused by the organic matter decay and is also relevant to the advection of low-DO water from the nearshore region. The DO supplement is primarily due to weakened stratification. Our analysis also shows that the minimum DO concentration in the nearshore region was extremely low in 1998, 2003, 2007 and 2010, related to El Niño signal in these summers.

Key words: dissolved oxygen, low-DO, Changjiang River Estuary, interannual variations, dual-core

Citation: Liu Anqi, Zhou Feng, Ma Xiao, Zhao Qiang, Liao Guanghong, Zhou Yuntao, Tian Di, Ni Xiaobo, Ding Ruibin. 2024. Inter-annual variations of dissolved oxygen and hypoxia off the northern Changjiang River (Yangtze River) Estuary in summer from 1997 to 2014. *Acta Oceanologica Sinica*, 43(6): 119–130, doi: 10.1007/s13131-023-2244-0

1 Introduction

Oxygen in seawater, namely dissolved oxygen (DO), functions as an important parameter for the survival of most organisms in the ocean (Brewer and Peltzer, 2009; Diaz and Rosenberg, 2008; Wishner et al., 2018). DO concentrations below 2 mg/L or 62.5 $\mu\text{mol/L}$ are usually defined as hypoxia in aquatic environments (Conley et al., 2009; Diaz, 2001; Guo et al., 2020; Paerl et al., 1998; Rabotyagov et al., 2014; Renaud, 1986; Wang et al., 2012;

Zhou et al., 2010; Zhu et al., 2011) but there are also a large number of studies using ~ 3 mg/L or higher values (Diaz and Rosenberg, 1995; Dai et al., 2006; Chen et al., 2007; Zhou et al., 2020). This hypoxia threshold is relatively stringent as 2 mg/L is much lower than the DO thresholds required for survival of many organisms (Vaquer-Sunyer and Duarte, 2008). Paerl et al. (1998) instead used 4 mg/L as a hypoxia threshold because this concentration would affect the survival of fish, mussels and inverteb-

Foundation item: The National Key Research & Development Program of China under contract No. 2023YFC3108003 in Project No. 2023YFC3108000; the National Natural Science Foundation of China under contract No. 41876026; the Scientific Research Fund of the Second Institute of Oceanography, Ministry of Natural Resources under contract No. YJJC2201; the National Programme on Global Change and Air–Sea Interaction Phase II under contract No. GASI-01-CJK; the Zhejiang Provincial Ten Thousand Talents Program under contract No. 2020R52038; the Project of State Key Laboratory of Satellite Ocean Environment Dynamics under contract No. SOEDZZ2105.

*Corresponding author, E-mail: zhoufeng@sio.org.cn; maxiao@sio.org.cn

rates. Recent studies suggest that fish generally require a higher DO concentration than crustaceans and echinoderms, while annelids and mollusks are less and least sensitive, respectively (Carstensen et al., 2014; Gray et al., 2002).

As one of the most famous eutrophication and hypoxia systems in the world, summer hypoxia in the Changjiang River Estuary (CJE) have attracted much attention (Chen et al., 2020; Wei et al., 2021b). The formation and evolution of seasonal hypoxia off the CJE have been investigated in many studies (Li et al., 2002; Zhang et al., 2007; Zhou et al., 2009). It is believed that the hypoxia first forms in June along the southern Zhejiang coast, then gradually spreads northward and splits into northern and southern parts (Li et al., 2002; Zhou et al., 2010). The hypoxia extent usually peaks in August, and gradually declines from September to November (Wang, 2009; Wei et al., 2015). In addition to seasonal variations, hypoxia in the CJE also shows large inter-annual variations (Ma et al., 2022; Ning et al., 2011). Since hypoxia was first recorded in the summer 1959, hypoxia in the CJE has occurred almost every year in the recent decades (Li et al., 2011; Lu et al., 2017; Luo et al., 2018; Qian et al., 2017; Zhang et al., 2016, 2019; Zhou et al., 2020; Zhu et al., 2017). The probability of hypoxia occurring in summer is about 60% before 1980s and increases to about 90% after the 1990s with all hypoxic events greater than 5 000 km² in the late 1990s and thereafter (Wang, 2009). And the hypoxic extent along the 32°N section tends to expand eastward from 1975 to 1995 (Ning et al., 2011). Recent study revealed that there are large differences in both DO concentration and rate of change along the section from nearshore to offshore in the northern CJE. The nearshore section often has a hypoxic core at the sea bed, where the concentration of DO is lower than 3 mg/L and has a much-stronger decreasing trend in 1997–2014 (Ma et al., 2022) than that during 1975–1995 (Ning et al., 2011). In contrast, the offshore part of the section has a core of low-DO-concentration, where the mean DO concentration is around 3–4 mg/L with a slightly increasing trend at the surface but a decreasing trend at the sea bed. However, it was not explained why these two cores differ in their long-term trends.

Numerous factors in combination with physical, biological, chemical, and sedimentary processes are likely responsible for the development and seasonal variability of hypoxia off the CJE (Guo et al., 2020; Luo et al., 2018; Wang et al., 2022, 2023; Zhang et al., 2021; Zhou et al., 2021a; Zhu et al., 2017). Water column stratification and eutrophication-induced high primary productivity are thought to be the two major factors contributing to the inter-annual variations and long-term trend of hypoxia (Chen et al., 2017; Gong et al., 2017; Obenour et al., 2012; Wei et al., 2019). Zhang et al. (2020) suggested that sediment oxygen consumption (SOC) is probably another important factor in the inter-annual variability (2008–2013) of hypoxia. By applying a state-of-the-art benthic-pelagic model coupled with a physical-biogeochemical model to the East China Sea (ECS), Meng et al. (2022) indicated that SOC is dominated by either advective flux of porewater or diffusive flux by bioturbation and its contribution to hypoxia ranges from ~15% to ~80%, but SOC is not the major factor responsible for interannual variations of hypoxia in this area (Zhou et al., 2021b). A recent modeling study suggests that the extent and magnitude of hypoxia off the CJE is largely modulated by the water with low-DO-concentration and low N/P ratio from the Kuroshio (Tian et al., 2022). In the short-term scale, previous studies suggest that a typhoon could attenuate the hypoxia event by increasing mixing, but would facilitate the subsequent hypoxia event by enhancing nutrient replenishment (Ni et al., 2016). Meng et al. (2022) found that typhoon-induced advection

could suppress upwelling in certain hypoxic zones and transport hypoxic water southward, resulting in a much lower DO concentration in the southern region than that before the typhoon passage. In the long-term scale, Ma et al. (2022) revealed that increasing hypoxia in summer could be exacerbated by excess freshwater runoff associated with El Niño event. In the history of hypoxia research in the CJE, another focus was on the division of the horizontal hypoxic extent into a northern and southern regions, which referred to the existence of a hypoxic center in the north of the CJE and the other one along the northern coast of Zhejiang Province (Li et al., 2002; Zhang et al., 2007; Zhou et al., 2009). Compared to the southern region, the northern region has a larger hypoxic extent and lower DO concentration (Zhou et al., 2010; Zhu et al., 2011). However, previous studies on the hypoxia in the northern region mainly focused on the nearshore region (approximately the region between 10–30 m isobath outside the CJE), but less on the offshore regions at the eastern edge of the cross-shelf section. The offshore region might be a potential hypoxic zone since the survey data in 2013 showed DO less than 3.5 mg/L between 32°–33°N at 124°E in the northern CJE (Wei et al., 2021a). There is a lack of a study of the long-term change mechanism in these two areas.

In this study, we aimed to reveal the interannual variations and trend of two low-DO cores with the nearshore core on the left and the offshore core on the right in a repeatedly-surveyed section with more hydrographic parameters than before from 1997 to 2014. To better understand the changes in the two low-DO cores and their formation mechanisms, we also analyzed the trend of stratification strength and phytoplankton biomass in the study region.

2 Data and method

2.1 Study area

The CJE is a large-river estuarine ecosystem where huge volumes of fresh water from the Changjiang River (approximately 28 900 m³/s) interact, and mix with sea water in the Yellow Sea and ECS to form a large river plume, namely the Changjiang River Diluted Water (CDW). The CDW spreads a considerable amount of nutrients from the river (nitrogen, phosphorus and silicon) along with the less-saline water into the transition zone, creating multiple fronts off the estuary (Li et al., 2021), which in turn leads to a highly productive region year-round and one of the largest seasonal hypoxia in the world during summer (Chen et al., 2007). The hydrographic features in the estuary in summer are strongly influenced by the interaction of the CDW with the local circulation (Fig. 1), e.g., the Taiwan Warm Current (TWC), which is a mixture of the Kuroshio intruded water and shelf water, the Yellow Sea Coastal Current (YSCC), the Jeju Warm Current (JWC), the Yellow Sea Cold Water Mass (YCWM), the Ji-angshu Shoal Current (JSC) and the Zhe-Min Coastal Current (ZMCC) (Lie et al., 2000; Park et al., 2011; Su and Huang, 1995; Wu et al., 2011; Xuan et al., 2012; Zhang et al., 2008; Zhou et al., 2017; Zhu et al., 2016). Section S1, northeast of the CJE, was sampled at 7 sites, i.e., S1a–S1g, located between latitude 31°N and 34°N and longitude 122°E and 126°E. Measurements were carried out in August in most years from 1997 to 2014, except in September in 2002 and 2004. Sampling sites in each section are evenly spaced at approximately 0.5° intervals.

2.2 Observational data

Temperature, salinity, dissolved oxygen (DO), nitrate (NO₃⁻-N), and phosphate (PO₄³⁻-P) were monitored by the

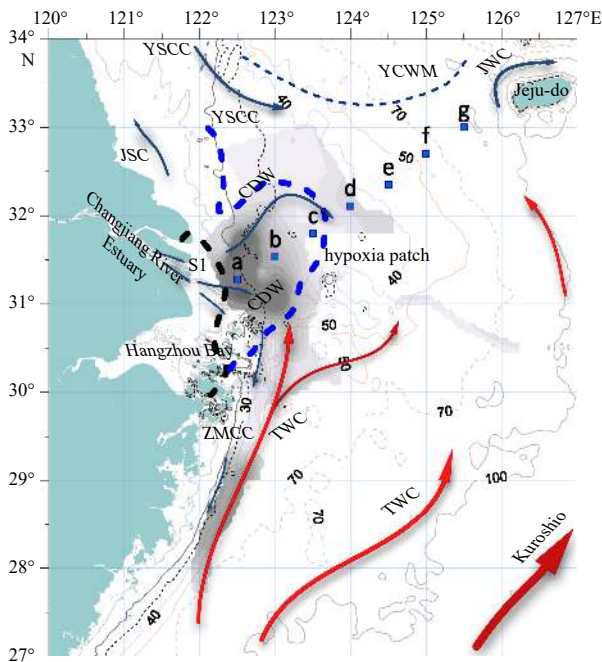


Fig. 1. Map of Section S1 in summer from 1997 to 2014 in the East China Sea and Yellow Sea with station number above marker. Gray shading indicates locations where hypoxia was found during historical surveys. The dashed black curve indicates the surface suspended sediment front near the Changjiang River mouth and dashed blue curve indicates the surface plume front (Li et al., 2021). The arrows indicate the direction of the summer circulation, and the red arrow represents the current, i.e., the Kuroshio and its branches, namely the Taiwan Warm Current (TWC), and the blue represents the current system with the nature of offshore water masses, including the Changjiang River Diluted Water (CDW), the Yellow Sea Coastal Current (YSCC), the Jeju Warm Current (JWC), the Yellow Sea Cold Water Mass (YCWM), the Jiangsu Shoal Current (JSC) and the Zhe-Min Coastal Current (ZMCC).

Ningbo Marine Environment Monitoring Center, Ministry of Natural Resources. Temperature and salinity were measured using a Sea-Bird model 911 conductivity-temperature-depth recorder (CTD) and DO was measured on board the vessels immediately after collection using the Winkler titration method. Water samples were collected at the surface, 5 m, 10 m, 15 m, 20 m, 25 m, 30 m, 50 m, 75 m, and at the bottom, which is typically 2–3 m above the sediment, using Niskin bottles (Table S1). The quality control of data has been completed by the Ningbo Marine Environment Monitoring Center and is widely used for ECS data assimilation (Zhao et al., 2015). More details can be checked in Ma et al. (2022).

In addition, a locally modified chlorophyll *a* (LMC) data set from Hao et al. (2019) was used to examine the influence of primary productivity on low DO. The LMC dataset is based on empirical modification of the OC-CCI (Ocean Colour Climate Change Initiative) standard products and also combined with *in situ* chlorophyll datasets for correction.

2.3 Trend analysis

The Mann-Kendall statistical test and Sen's slope estimator, a widely-used method for time series analysis in hydrographic and meteorological data, were used to derive the long-term trend (Wang et al., 2013). The advantage of this method is that the data

need not be normally distributed (Akritas et al., 1995; Mann, 1945; Sen, 1968; Theil, 1992) because our data are not that long. For each measurement point on the section measured for 18 a, Sen's slope estimator was first used to calculate the trend, and then the standard normal test statistic Z_{MK} was obtained by the Mann-Kendall statistical test to assess the significance of the trend. The significance level $\alpha = 0.05$, $Z_{1-\alpha/2} = Z_{0.975} = 1.96$ was chosen for the test.

2.4 Detection of the extreme years

Hypoxia in the CJE is partly influenced by human activities and climate change (Chen et al., 2020). During 1997–2014, there were many extreme weather events that may affect the hypoxia of the CJE, such as the catastrophic flood in 1998 (Wan et al., 1999) and the heat wave in 2003 (Wang et al., 2006), etc. Meanwhile, historical observations have shown a large inter annual variability of the hypoxic zone in the estuary (Zhou et al., 2020). Therefore, the observation data may contain unusually low or unusually high values that could affect the results of interannual variations. Such values are called outliers and need be identified. It is also necessary to analyze the cause of these outliers. The years that contain the outliers are referred to as extreme years in this study. The boxplot method, the most common method for testing extreme values (Sun et al., 2010; Wang and Su, 2019), was used to identify the outliers in our data. The boxplot method has the advantage of being able to work with data that do not conform to normal distribution. In the study, multipliers other than the whisker 1.5 were used to filter out outliers (Frigge et al., 1989).

2.5 Parameters related to the low DO

The threshold for hypoxia varied in earlier studies, ranging from 2 mg/L to 4 mg/L (Diaz, 2001; Karim et al., 2003; Paerl, 2006). In this study, the threshold for low DO was defined as 4 mg/L (Yin et al., 2004) and for hypoxia as 3 mg/L (Dai et al., 2006; Zhou et al., 2020). The nearshore core is designated as the range from 20 m to the bottom at 122.5°–123.5°E, and the offshore core as the range from 30 m to the bottom at 123.5°–124.5°E (Li et al., 2002; Wei et al., 2007). The thickness of the low-DO water is defined as the difference between the maximum depth and the minimum depth at which low DO occurs. Time series of data, i.e., DO solubility, apparent oxygen utilization (AOU), stratification strength, CDW strength and primary productivity, are created to assess the effect of physical and biological processes on DO along Section S1. The AOU is the difference between the observed DO concentration and equilibrium saturation concentration in water using the same-layer temperature and salinity (Ning et al., 2011). The density difference between bottom and surface water ($d\rho$) is used to represent stratification strength, one of the key physical variables for the formation of hypoxia (Li et al., 2002; Wei et al., 2007). The water mass on Section S1 with salinity <30 is referred to as CDW (Chi et al., 2020; Su et al., 1996; Zhu et al., 2011). The CDW strength at the nearshore core is defined as the area of the CDW between Stations S1a–S1c (the length of Section S1 is 341 km). The CDW strength at the offshore core was determined as the area of the CDW between Stations S1c–S1e. Primary productivity, which produces organic material that consumes DO, is roughly represented by Chl-*a* concentration in the study. The integral re-average of high Chl-*a* concentration (> 5 $\mu\text{g/L}$) between 31°–32°N and 122.5°–123.5°E is defined to calculate the primary productivity of the nearshore region. The integral re-average of high Chl-*a* concentration (> 5 $\mu\text{g/L}$) between 31°–32°N and 123.5°–124.5°E is determined to estimate the primary productivity of the offshore region. Since phytoplankton bloom and hypoxia have a time lag of around 1–4 weeks in the region (Zhou

et al., 2020), the average Chl-*a* of the early month is utilized to represent the primary productivity leading to hypoxia in the present month. That is, the average Chl-*a* data in July were used in all the years except 2002 and 2004, when the average Chl-*a* data in August used since observations were only available in September.

3 Results

3.1 Vertical structure and variation of DO concentration

Figure 2 shows two separate low-DO cores along the section. The low DO in the nearshore region is more severe in trend and frequency than that in the offshore region. The nearshore core is located at the western end of Section S1 at depth higher than 20 m, and the offshore core is located in the middle of Section S1 at a depth of > 40 m, or on the eastern side of the submerged valley near the isobaths from 30 m to 40 m in the southeastern area off the CJE. The lowest DO in these two cores are 0.77 mg/L and 0.51 mg/L, respectively. The trend in the nearshore core [-0.07 mg/(L·a)] is more pronounced than that in the offshore core (no clear trend), as shown in Fig. 2a. The descending trend of DO in the nearshore core is greater than the mean rate of -0.023 mg/(L·a) in period of 1975–1995 (Ning et al., 2011). The largest frequency of low-DO is 14 times (approximately 78%) at 122.5°E in the nearshore core, followed by 10 times (approximately 56%) at 124.5°E in the offshore core (Fig. 2b), which is different from their geometric centers of the two low-DO cores in about 123°E and 124°E . During the period, the nearshore low-DO core is relatively stable and remains in 122.5°E – 123.5°E , while the offshore low-DO core moves back and forth between 123.5°E – 125°E . The movement of these two cores is caused by the significant interannual variations of water masses, which are likely associated with large-scale horizontal advection driven by the shelf circulation and local factors related to vertical mixing and primary production (Fig. S1). It is noted that DO profile is fairly complicated in the vertical structure, which exhibits an increasing trend at around 10-m depth of the nearshore region at 122.5°E [0.07 mg/(L·a)] and also at around 5-m depth at 123.5°E – 124.5°E [0.04 mg/(L·a)], but a decreasing trend [-0.06 mg/(L·a)] at 8-m depth and shallower at 122.5°E – 123.5°E and an increasing trend [0.1 mg/(L·a)] from ~15 m to the bottom at 125.5°E .

In addition to the frequency of low DO, the thickness of two low-DO cores and the lowest DO are also important parameters

to be examined. Influenced by different water masses in the nearshore and offshore regions (Fig. S2), the changes in the thickness and the minimum DO of these two low-DO cores are also different. For the nearshore core, the low-DO thickness ranges from 9 m to 32 m with a rising rate of 0.43 m/a and the minimum DO concentration range is 0.77–4.90 mg/L with a decreasing rate of -0.07 mg/(L·a) (Figs 3a and b). Comparatively, the offshore low-DO core has a thickness ranging from 5 m to 41 m with a falling rate of -1.55 m/a and the minimum DO concentration there fluctuates between 0.51–5.96 mg/L with no obvious rate (Figs 3c and d). Although the two low-DO cores have many different characteristics, they both show a significant negative correlation between the thickness of low-DO and the minimum DO concentration ($r = -0.85$, $p < 0.01$ for the nearshore core; and $r = -0.73$, $p < 0.01$ for the offshore core). That is, the greater the low-DO thickness, the lower the minimum DO concentration. It can be seen that low-DO thickness and the minimum DO concentration at both regions present significant inter-annual variations besides the long-term trend, implying probable influences of several factors, such as three-dimensional circulation and velocity shear in the vertical (Zhou et al., 2020).

3.2 Variation of summer environmental factors

The AOU has similar spatial characteristics to DO, while temperature, salinity, σ_t density, nitrate, and phosphate concentrations differ from those of DO due to the interaction of various water masses in the northern CJE. The trend and values of temperature, salinity, and σ_t density averaged over the period are analyzed using Mann-Kendall's statistical test and Sen's slope estimation. For the nearshore low-DO core, the change in salinity dominates the density change, while for the offshore core, both the temperature and salinity changes dominate the density change (Figs 4a–c). The profile of density averaged over the period is similar to that of salinity for the entire section. Temperature, salinity, and density of the nearshore core all show a downward trend, indicating that salinity has a greater influence on density than temperature. The density of the nearshore surface water shows a stronger downward trend [-0.13 kg/($\text{m}^3\cdot\text{a}$)] than that of the nearshore bottom water [-0.02 kg/($\text{m}^3\cdot\text{a}$)]. Thus, the increasing density difference between surface and bottom causes an upward trend in the stratification of the nearshore region. In contrast, the density of the offshore surface water [0.05 kg/($\text{m}^3\cdot\text{a}$)] shows a rising trend opposite to that of the bottom water

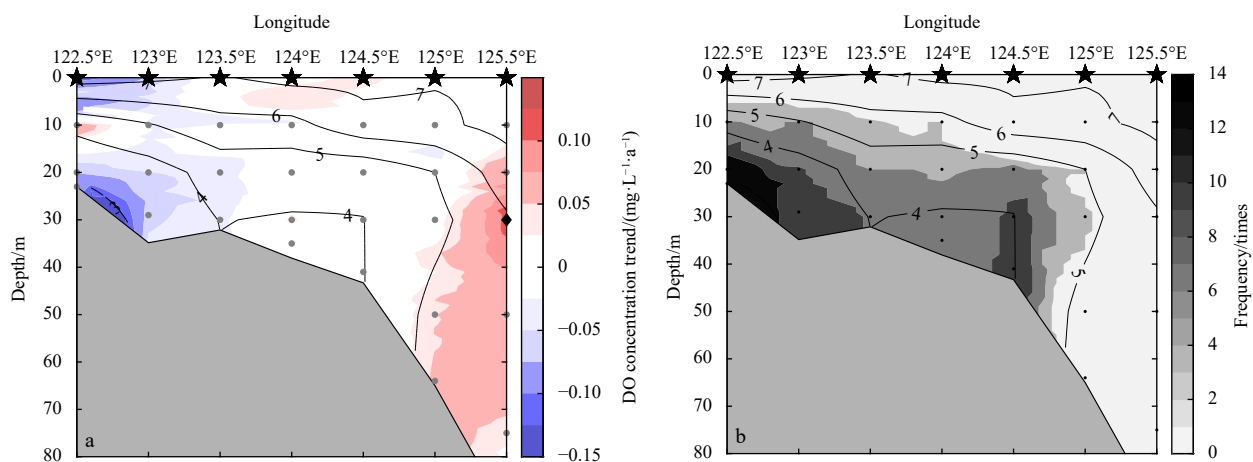


Fig. 2. Eighteen-year averaged DO concentration in summer. a. Trend of DO concentration; b. frequency of low DO. The isoline represents the averaged DO concentration, the shading represents the trend (a) and frequency (b) of low DO, the black dot with five-pointed star indicates the sampling location, and the black dots are the sampling point.

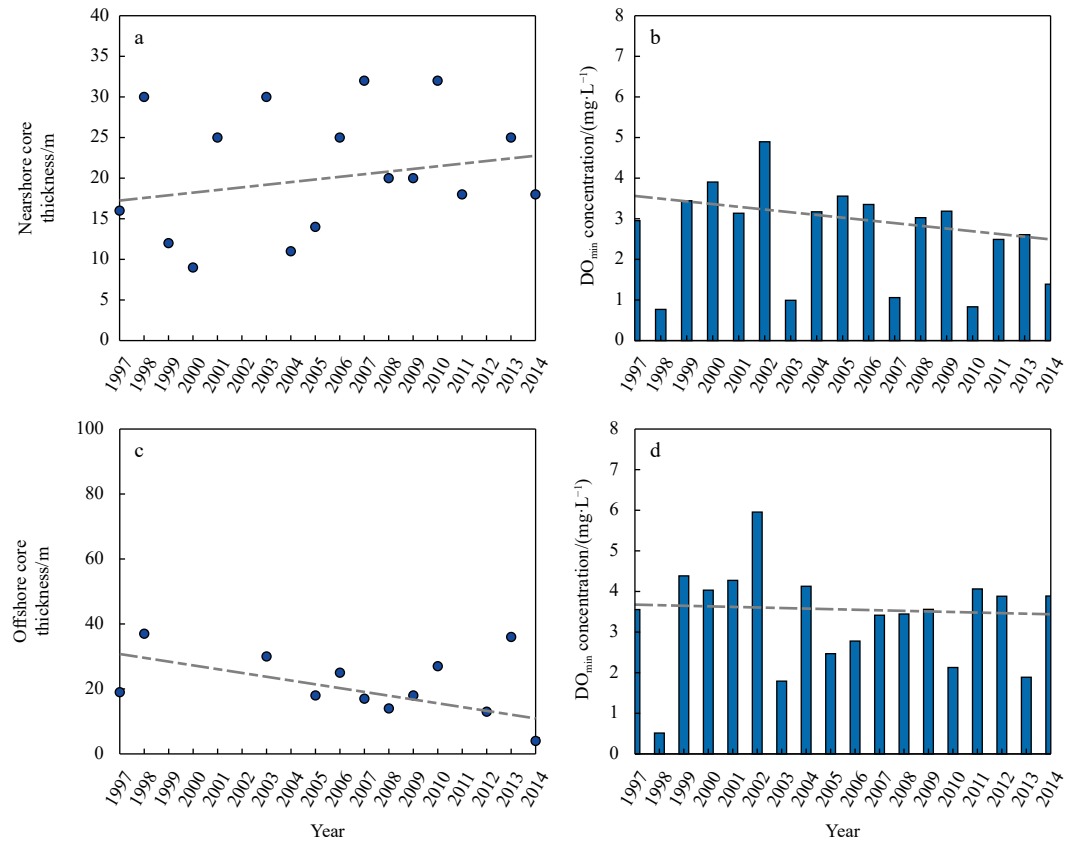


Fig. 3. Variations in DO-relevant parameters. a, c. The thickness of the low-DO core (DO concentration < 4 mg/L) in the nearshore and offshore regions along Section S1; b, d. the minimum DO concentration in the two low-DO cores along Section S1. The top two panels are the result of the nearshore core and the bottom panels are the result of the offshore core. The gray dash lines represent the trend calculated using Sen's slope estimator. The thickness of low-DO core is represented by subtracting the minimum depth from the maximum depth of the core where the DO concentration is less than 4 mg/L.

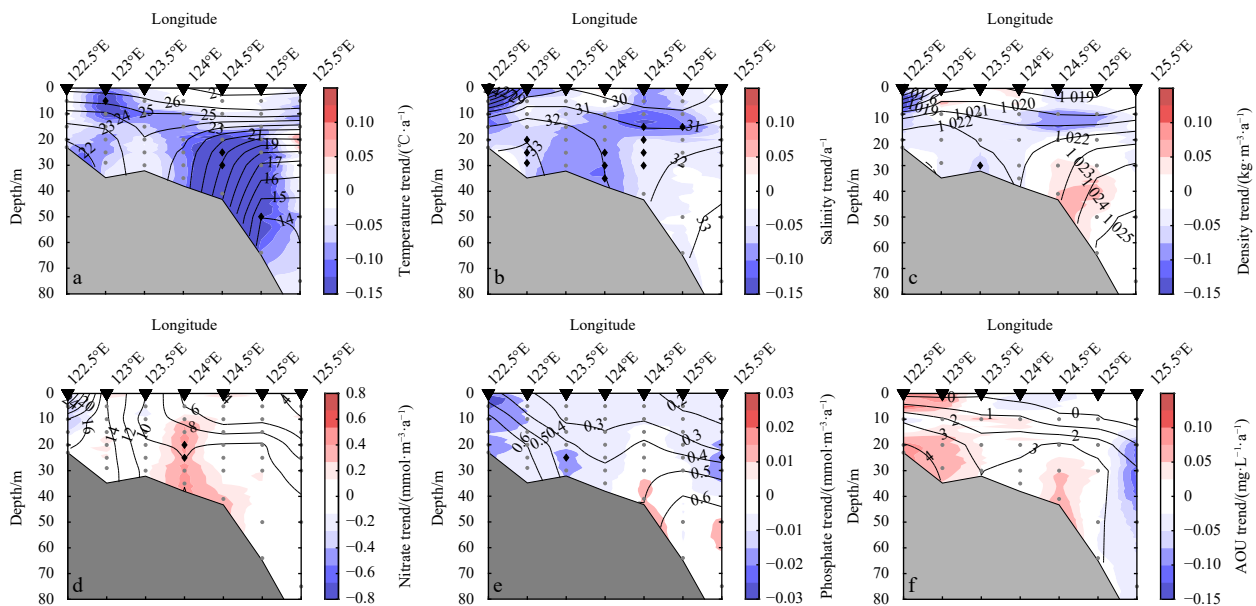


Fig. 4. Eighteen-year averages of environmental factors in summer; temperature (a), salinity (b), density (c), nitrate concentration (d), phosphate concentration (e), and apparent oxygen utilization (AOU) (f) in Section S1. The isoline represents the average distribution of hydrographic variables, the shading represents the trend calculated using Mann-Kendall method, the black diamond indicates that the station location is significant with 95% confidence, the gray dot was not significant with 95% confidence, and the black triangle was the sampling site.

[$-0.01 \text{ kg}/(\text{m}^3 \cdot \text{a})$], and the decreasing density difference between surface and bottom causes a downward trend in the stratification at the offshore region. As seen in the salinity and density profiles, a pronounced CDW with low salinity (<30) and low density ($<1019 \text{ kg}/\text{m}^3$) is distributed off the CJE from surface to 10 m at $122.5^\circ\text{--}123.5^\circ\text{E}$ (Figs 4b and c), forming a fairly strong stratification over two low-DO cores. Based on the current system in the CJE (Fig. 1), it could be inferred that the higher temperature, salinity and density at the nearshore bottom are likely associated with the TWC intrusion (Qi, 2014). Figs 4d–f show the high nitrate ($>10 \text{ mmol}/\text{m}^3$) and phosphate ($>0.4 \text{ mmol}/\text{m}^3$) content correspond to the high AOU value ($>3 \text{ mg}/\text{L}$), indicating that oxygen consumption by biological processes has an important influence on the decline of DO. Nitrate concentration is highest in the nearshore surface layer ($>24 \text{ mmol}/\text{m}^3$), second highest in the nearshore layer below the surface ($>14 \text{ mmol}/\text{m}^3$), and gradually decreases along the section to the offshore region (Fig. 4d). Phosphate content is high in the nearshore region and the offshore bottom region but low in the offshore surface region (Fig. 4f). The nutrient distribution is largely influenced by the high-nitrate-concentration CDW (Wang and Cao, 2012; Zhou et al., 2008) and the high phosphate content brought by the TWC (Ding et al., 2019). Interestingly, phosphate shows different trends from nitrate, with a general distinctive downward trend west of 123.5°E and a weak downward trend for upper layer water in the offshore region, but an upward trend at the bottom of $124.5^\circ\text{--}125.5^\circ\text{E}$. The AOU has two high-concentration cores ($>3 \text{ mg}/\text{L}$) similar to those in DO concentration. The two cores show an upward trend in

AOU concentration [$0.08 \text{ mg}/(\text{L} \cdot \text{a})$ and $0.06 \text{ mg}/(\text{L} \cdot \text{a})$], consistent with the downward trend in DO concentration. The surface AOU also shows an increasing trend, which is responsible for the decreasing trend of the surface DO.

3.3 Roles of stratification and primary productivity

Although stratification and primary productivity are two important factors responsible for the development of hypoxia, the nearshore core differs greatly from the offshore one in both DO concentration and relevant hydrographic parameters as shown in Figs 2–4. A closer examination of stratification and primary productivity reveals two distinct regimes for the two low-DO cores. In the nearshore region, stratification ranges from $1.0 \text{ kg}/\text{m}^3$ to $11.5 \text{ kg}/\text{m}^3$ with an increasing trend of $0.07 \text{ kg}/(\text{m}^3 \cdot \text{a})$ (Fig. 5a). In this area as well, there is a weak negative correlation (gray line, $n = 17$, $r = -0.45$, $p = 0.07$) between the minimum DO concentrations and stratification as shown in Fig. 5b. The insignificance of this correlation could be explained by the existence of unaccounted-for other components. Zhu et al. (2011) found that the linear relationship between DO depletion and stratification would not hold for stratification above a certain range. As a result, the minimum DO concentration and stratification in the nearshore area have a significant negative connection (black line, $n = 15$, $r = -0.55$, $p < 0.05$) when years (1999 and 2003) with stratification more than $10 \text{ kg}/\text{m}^3$ are excluded. Additionally, the AOU increases (Fig. 4f), which is another indication of the effects of increased stratification on the decrease in DO concentration. In contrast, Fig. 5c shows an increasing trend in primary productivity

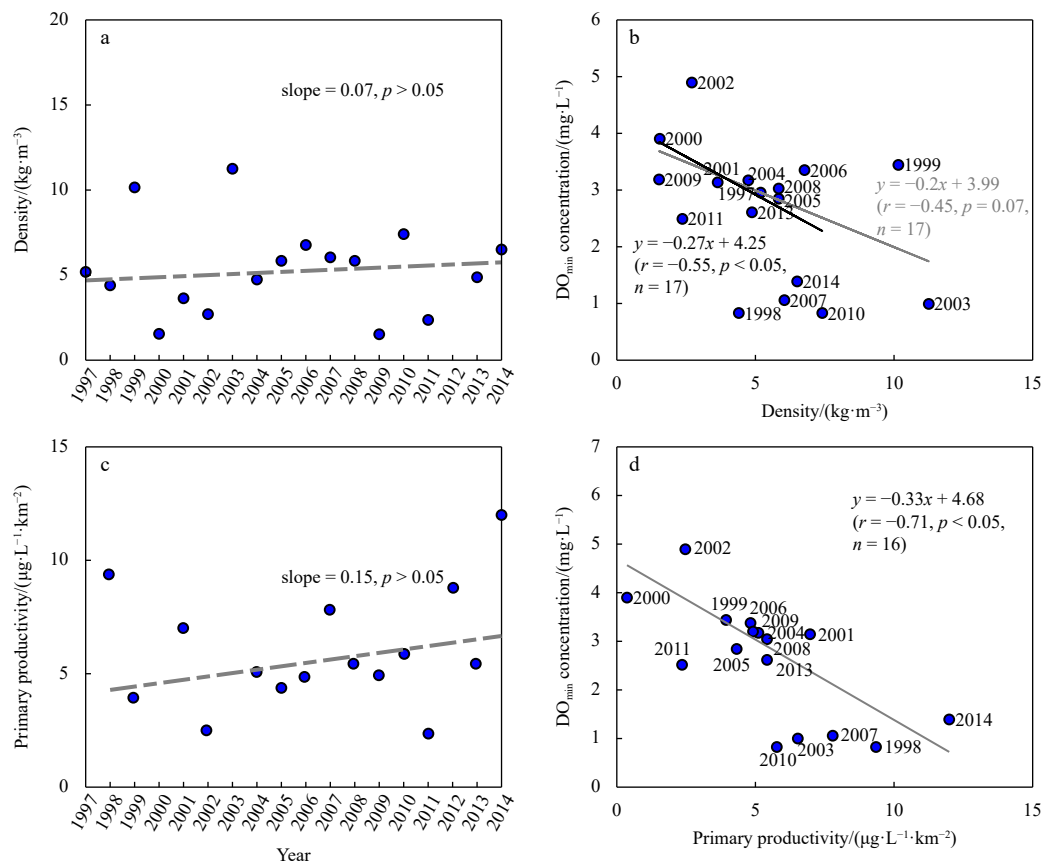


Fig. 5. The trend in density stratification and primary productivity (a, c) in the nearshore region. Correlations of minimum DO and stratification and primary productivity (b, d) in the nearshore region. The gray line and words in b denote the correlations of minimum DO and stratification in 17 a, and the black line and words in b denote the correlations of minimum DO and stratification in 15 a (except for 1999 and 2003).

($0.15 \mu\text{g}/(\text{L}\cdot\text{km}^2\cdot\text{a})$), which is consistent with the upward trend in AOU in the nearshore region. Also, in Fig. 5d, there is a high negative correlation between the lowest DO concentration and primary productivity ($r = -0.71, p < 0.05$). The upward trend of primary productivity is consistent with the result reported by Chen et al. (2017) and may explain the declining trend of nitrate concentration in the nearshore region (Figs 4d and f).

Trend and correlation analyses were also applied to the offshore core shown in Fig. 6. The stratification shows a downward trend ($-0.02 \text{ kg}/\text{m}^3$) with large interannual variations in the offshore (Fig. 6a). The scatter diagram of the observed stratification and minimum DO (Fig. 6b) shows that there is a good negative correlation between the minimum DO concentration in the offshore core and stratification ($n = 17, r = -0.7, p < 0.05$). There is no clear trend for primary productivity in the offshore region and the correlation between minimum DO concentration and primary productivity is insignificant (Figs 6c and d). In short, the relationship between offshore primary productivity and minimum DO is uncertain because the primary productivity has a high value only in 1998 and 2003. Moreover, there is a high positive correlation of the minimum DO concentration between the nearshore and offshore cores ($r = 0.67, p < 0.05$).

4 Discussion

Previous studies have shown that a large nearshore hypoxic zone with a few patch-like offshore hypoxic zones is distributed off the CJE with large interannual variations (Chi et al., 2020; Li et al., 2002; Ma et al., 2022; Wei et al., 2007, 2021a; Zhou et al., 2009; Zhu et al., 2011). This study suggests a dual-core structure

at the bottom of the northern CJE. However, the bottom DO in the two cores is different from each other (Table S2). The nearshore low-DO core has become severe with the lowest DO concentration descending at a rate of $0.07 \text{ mg}/(\text{L}\cdot\text{a})$ and the thickness of low-DO water rising at a rate of $0.43 \text{ m}/\text{a}$. The nearshore minimum DO shows a trend consistent with that of Ma et al. (2022) and significantly larger than the rate of $0.023 \text{ mg}/(\text{L}\cdot\text{a})$ from Ning et al. (2011). This result also suggests that the minimum DO concentration is not only an important indicator of marine organism survival, but can also be used as a means to assess the severity of hypoxia. In contrast, the location of the offshore low-DO core is not stable. In the offshore region, the minimum DO concentration shows large interannual fluctuations and the thickness of low-DO water is falling at a rate of $-1.55 \text{ m}/\text{a}$. Compared to the trend estimated by Ma et al. (2022), the Mann Kendall statistical test and Sen's slope estimate used in this study are more accurate than the T -test when processing data that do not quite meet the requirements of normal distribution (six groups of measurement points are non-normally distributed). In addition, the hydrographic characteristics of temperature, salinity, density, and phosphate show that the low-DO in this section may be influenced by CDW, TWC, YSCC, JWC, YCWM (Fig. S2), and the local oxygen consumption process (Fig. 4). Density stratification and organic matter decomposition are believed to be the two fundamental factors leading to low DO (Zhang et al., 2020), and they also have a good correlation with the nearshore minimum DO concentration (Figs 5b and d). The results show significant differences between the offshore core and the nearshore core. Meanwhile, the minimum DO of the offshore core is

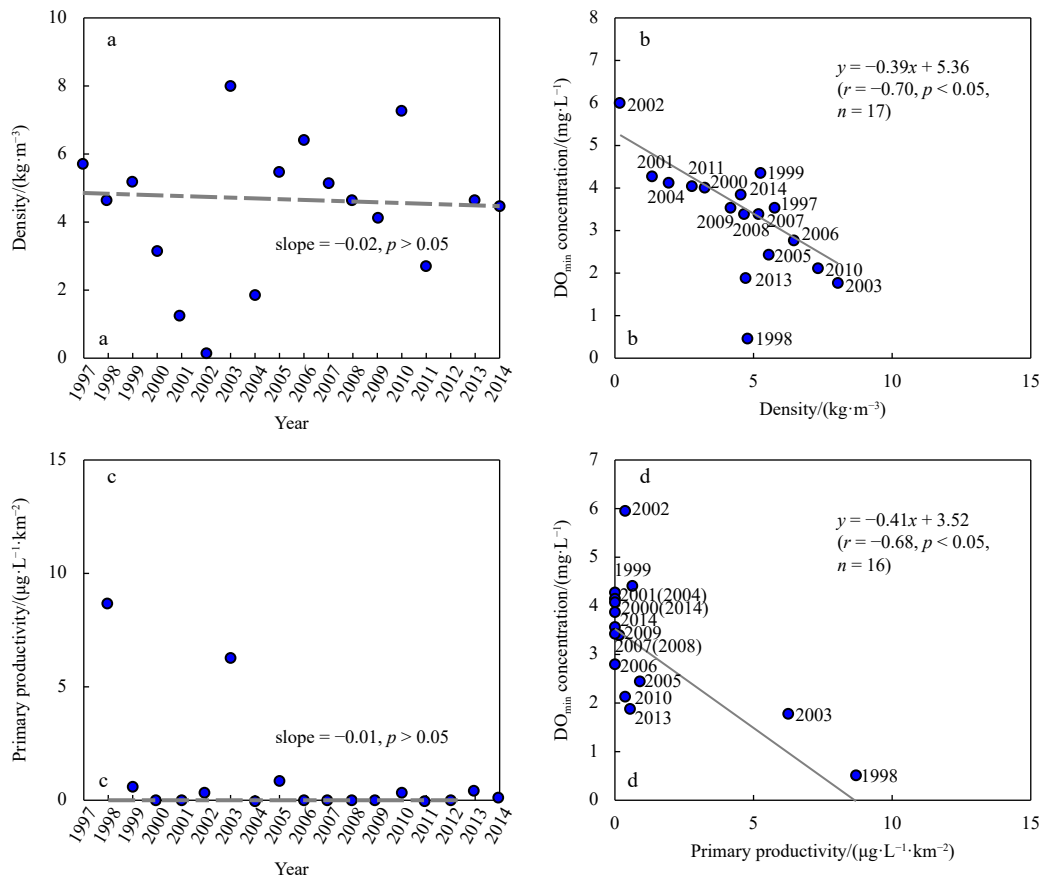


Fig. 6. Trend of stratification and primary productivity (a, c) in the offshore core. Correlations of minimum DO and stratification and primary productivity (b, d) in the offshore core.

strongly correlated with that of the nearshore core. Therefore, the mechanisms responsible for the two low-DO cores are discussed below.

4.1 Formation of the trend in the nearshore low-DO core

As shown in Figs 5a and b, stratification in the nearshore core shows an increasing trend [$0.07 \text{ kg}/(\text{m}^3 \cdot \text{a})$] and is negatively correlated with the minimum DO concentration ($r = -0.55, p < 0.05$). These results are consistent with previous studies suggesting that the formation and maintenance of the low DO is mainly due to enhanced stratification of seawater (Zhao et al., 2017). Previous studies have also shown that stratification in summer can be largely affected by CDW (Zhou et al., 2010). The CDW could bring much less-saline water and reduce the surface density. As shown in Fig. 4b, the salinity at the depth of 0–10 m in the nearshore region has a clear downward trend. Statistical analysis shows that the intensity of CDW intrusion is significantly positively correlated with the stratification of the nearshore core ($r = 0.73, p < 0.05$) and shows a slight upward trend (Figs 7a and b). This means that stratification increases as the CDW increases, which prevents the vertical exchange of DO from the surface to the sea bed. Su et al. (1996) found that the TWC has a significant upward trend and moves toward the coast near the bottom layer, and its frontal water may even reach 32°N in summer. As Figs 4a–c show, the nearshore bottom water with low temperature ($<23^\circ\text{C}$), high salinity (>32) and high density could originate from the TWC, which enhances stratification. In addition to physical processes, biogeochemical processes are also important for the development of low DO or even hypoxia. The nearshore core is located between the turbidity front and the plume front, and is characterized by high primary productivity around the CJE (Li et al., 2021). Primary productivity in the nearshore core shows an upward trend ($0.15 \mu\text{g}/(\text{L} \cdot \text{km}^2 \cdot \text{a})$), and is significantly negatively correlated with the minimum DO concentration. As shown in Fig. 4f, the AOU in the nearshore core shows an increasing trend. Together with increasing stratification, the increase in primary productivity causes the downward trend of the minimum DO.

Primary productivity in the upper layer of the nearshore region increases faster due to the large amount of nutrients brought by the CDW (Chen et al., 2017). At the same time, the continuous increase in primary productivity consumes a large amount of nutrients, resulting in a downward trend of nitrate and phosphate in the upper layer water of the nearshore region (Figs 4d and e).

4.2 Formation of the trend in the offshore low-DO core

The formation of the offshore low-DO core is different from that of the nearshore core. The minimum DO in the offshore core shows no obvious trend with large interannual variations. To investigate the large fluctuations, two relevant processes need to be analyzed, i.e., DO consumption and supply. The DO consumption mainly refers to the oxygen consumption of organic material (Chi et al., 2017; Zhu et al., 2011), which could be reflected in the AOU in the offshore bottom (Fig. 4f). Wei et al. (2021a) suggested that the northeastern CDW patch with low salinity, high nutrient content and phytoplankton contributes to the growth of hypoxia. Accordingly, decreasing stratification in the offshore region could explain why DO there did not decline during this period (Fig. 6). Further, the decrease in stratification intensity is probably caused by the anticyclonic circulation centered around ($31^\circ\text{N}, 124^\circ\text{E}$) that brought down the upper-layer water, increased the temperature, reduced the salinity, and reduced the density in the bottom (Wei et al., 2015; Zou et al., 2001). The decrease in stratification intensity means enhanced ventilation of DO, which could alleviate the hypoxia at the bottom. Therefore, the effect of the increase in AOU at the bottom is counteracted by the decrease in stratification in the vertical, leading to an unclear trend of the minimum DO concentration.

A schematic diagram illustrates the mechanism of the long-term trend of two low-DO cores in the northeastern CJE (Fig. 8). Our results indicate that bottom oxygen consumption causes two low-DO cores below the pycnocline along the section, namely the nearshore core and the offshore core. The increase in primary productivity and stratification over the nearshore core jointly enlarges the downward trend of the minimum DO in the nearshore region, while the weakening of seawater stratification over the offshore core relaxes the DO at the bottom.

4.3 Years with severe low-DO in the nearshore patch

From the analysis in Sections 3.1 and 4.1, it can be inferred that the descending trend in the nearshore minimum DO concentration is caused by the increase of stratification and primary productivity. But the interannual variations of the nearshore minimum DO concentration is much larger than the trend, which could be related to extreme weather or climate events in certain years. Four years (1998, 2003, 2007 and 2010) have abnormal signals according to the boxplot method (Fig. 9, hereafter referred to as extreme years). When these extreme years are excluded from trend analysis, the minimum DO concentration trend changes to

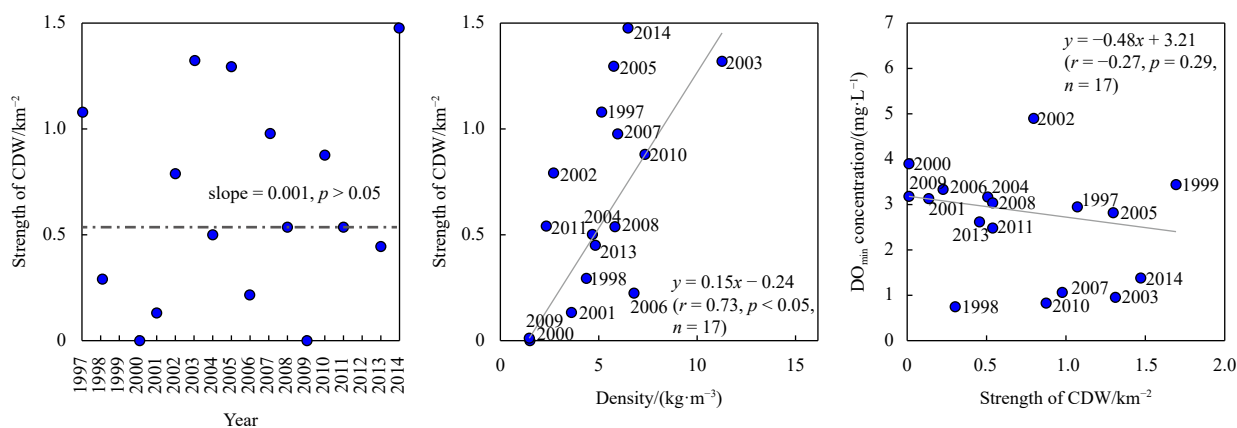


Fig. 7. The trend of CDW strength in the nearshore core (a), relation between stratification and CDW strength (b), relation between the minimum DO and strength of CDW in the nearshore core (c).

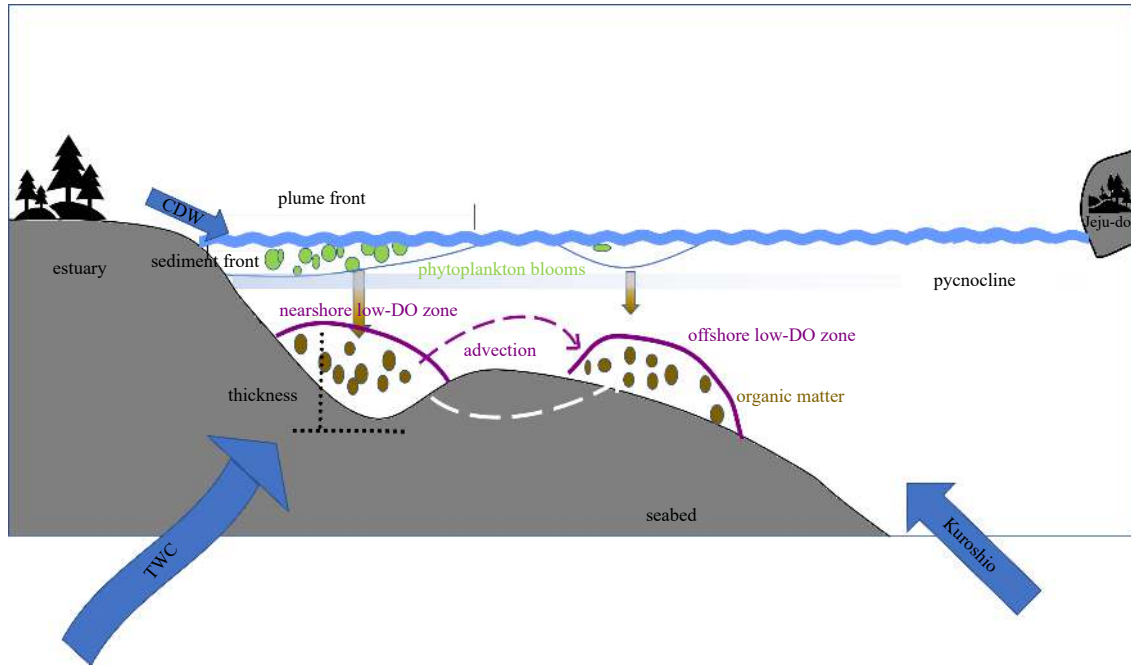


Fig. 8. Schematic diagram of physical and biogeochemical processes responsible for the formation of two low-DO cores along the section in the northern CJE.

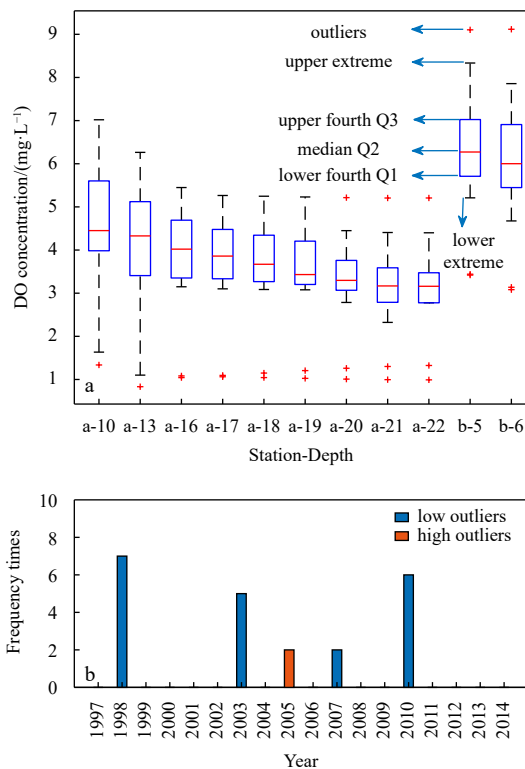


Fig. 9. Boxplot of the minimum DO in the nearshore core (a). Frequency of the year of outliers (red “+”) in a (b). Depth unit: m.

0.11 mg/(L·a) with confidence level higher than 95%. The minimum DO of these four extreme years (average 1.5 mg/L) is far below the low DO threshold (4 mg/L). This result is consistent with that of Ma et al. (2022), who assumed that low DO would be exacerbated in the El Niño decay summer (Fig. 10). There are three likely reasons for the worsening of low DO in the El Niño decay

summer. First, precipitation increased in the Changjiang River watershed due to the enhanced anticyclonic anomaly of moisture transport, resulting in the expansion of low salinity water and strengthening of stratification off the estuary. Second, the surface wind anomalies of the ECS continental shelf in July and August of such years tend to move northeastward than in normal years, which promotes the intrusion of the Kuroshio into the ECS shelf through the Ekman effect. Third, typhoons or tropical storms were absent or less frequent in El Niño decaying summers than in other years. This resulted in negative standard deviation anomalies of the SST and wind fields in the ECS, promoting the maintenance of stratification and oxygen depletion.

5 Summary

Based on long-term repeated sectional observations in the northern CJE from 1997 to 2014, DO and other hydrographic parameters are examined to estimate the multi-year average, trend, and frequency of low DO and to explore the mechanisms responsible for the formation and difference of the two low-DO cores. The trend and frequency of two low-DO cores (nearshore core and offshore core) differ from each other. The location of the nearshore low-DO core is relatively stable and the DO concentration shows a slight downward trend at an average rate of -0.07 mg/(L·a). The offshore low-DO core moves back and forth between 123.5° – 125.5° E with no clear trend. The formation processes of the two low-DO cores are different. The decreasing trend of DO at the nearshore low-DO core is primarily due to the increase in stratification and primary productivity. The fluctuating minimum DO concentration in the offshore core is likely due to competition and counteraction of DO consumption processes (respiration, nearshore water advection) and DO supply processes (weakening of stratification). Note that the sectional data have limitations in those four years (1998, 2003, 2007 and 2010) with extremely low minimum DO concentrations in nearshore waters are exceptional. These extremely low minimum DO concentrations are probably caused by El Niño relevant events.

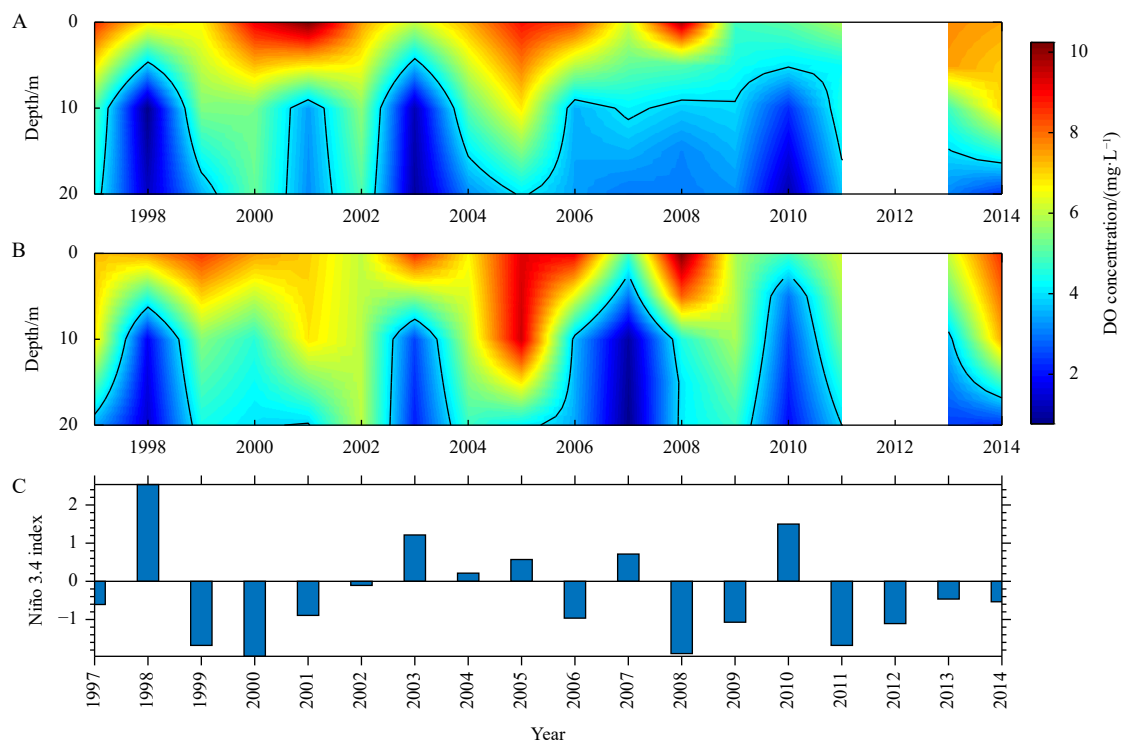


Fig. 10. DO concentration distribution at Station a (A) and Station b (B) from 1997 to 2014; the Niño 3.4 index from 1997 to 2014. The Niño 3.4 index data from [Ma et al. \(2022\)](#) (C).

References

- Akritas M G, Murphy S A, Lavalley M P. 1995. The theil-sen estimator with doubly censored data and applications to astronomy. *Journal of the American Statistical Association*, 90(429): 170–177, doi: [10.1080/01621459.1995.10476499](#)
- Brewer P G, Peltzer E T. 2009. Limits to marine life. *Science*, 324(5925): 347–348, doi: [10.1126/science.1170756](#)
- Carstensen J, Conley D J, Bonsdorff E, et al. 2014. Hypoxia in the Baltic Sea: biogeochemical cycles, benthic fauna, and management. *Ambio*, 43(1): 26–36, doi: [10.1007/s13280-013-0474-7](#)
- Chen C C, Gong G C, Shiah F K. 2007. Hypoxia in the East China Sea: one of the largest coastal low-oxygen areas in the world. *Marine Environmental Research*, 64(4): 399–408, doi: [10.1016/j.marenvres.2007.01.007](#)
- Chen Jianfang, Li Dewang, Jin Haiyan, et al. 2020. Changing nutrients, oxygen and phytoplankton in the East China Sea. In: Chen C T A, Guo Xinyu, eds. *Changing Asia-Pacific Marginal Seas*. Singapore: Springer, 155–178
- Chen Jianyu, Pan Delu, Liu Mingliang, et al. 2017. Relationships between long-term trend of satellite-derived chlorophyll-*a* and hypoxia off the Changjiang estuary. *Estuaries and Coasts*, 40(4): 1055–1065, doi: [10.1007/s12237-016-0203-0](#)
- Chi Lianbao, Song Xiuxian, Yuan Yongquan, et al. 2017. Distribution and key influential factors of dissolved oxygen off the Changjiang River Estuary (CRE) and its adjacent waters in China. *Marine Pollution Bulletin*, 125(1–2): 440–450, doi: [10.1016/j.marpolbul.2017.09.063](#)
- Chi Lianbao, Song Xiuxian, Yuan Yongquan, et al. 2020. Main factors dominating the development, formation and dissipation of hypoxia off the Changjiang Estuary (CE) and its adjacent waters, China. *Environmental Pollution*, 265: 115066, doi: [10.1016/j.envpol.2020.115066](#)
- Conley D J, Bonsdorff E, Carstensen J, et al. 2009. Tackling hypoxia in the Baltic Sea: is engineering a solution?. *Environmental Science & Technology*, 43(10): 3407–3411, doi: [10.1021/es8027633](#)
- Dai Minhan, Guo Xianghui, Zhai Weidong, et al. 2006. Oxygen depletion in the upper reach of the Pearl River estuary during a winter drought. *Marine Chemistry*, 102(1–2): 159–169, doi: [10.1016/j.marchem.2005.09.020](#)
- Diaz R J. 2001. Overview of hypoxia around the world. *Journal of Environmental Quality*, 30(2): 275–281, doi: [10.2134/jeq2001.302275x](#)
- Diaz R J, Rosenberg R. 2008. Spreading dead zones and consequences for marine ecosystems. *Science*, 321(5891): 926–929, doi: [10.1126/science.1156401](#)
- Diaz R J, Rosenberg R. 1995. Marine benthic hypoxia: A review of its ecological effects and the behavioural responses of benthic macrofauna. *Oceanography and Marine Biology: An Annual Review*, 33: 245–03
- Ding Ruibin, Huang Daji, Xuan Jiliang, et al. 2019. Temporal and spatial variations of cross-shelf nutrient exchange in the East China Sea, as estimated by satellite altimetry and *in situ* measurements. *Journal of Geophysical Research: Oceans*, 124(2): 1331–1356, doi: [10.1029/2018JC014496](#)
- Frigge M, Hoaglin D C, Iglewicz B. 1989. Some implementations of the boxplot. *The American Statistician*, 43(1): 50–54, doi: [10.1080/00031305.1989.10475612](#)
- Gong Songbai, Gao Aiguo, Ni Guantao, et al. 2017. Progress in research of hypoxia in estuaries and coastal areas in China. *Water Resources Protection (in Chinese)*, 33(4): 62–69, doi: [10.3880/j.issn.1004-6933.2017.04.010](#)
- Gray J S, Wu R S S, Or Y Y. 2002. Effects of hypoxia and organic enrichment on the coastal marine environment. *Marine Ecology Progress Series*, 238: 249–279, doi: [10.3354/meps238249](#)
- Guo Xiaoyi, Xu Bochao, Burnett W C, et al. 2020. Does submarine groundwater discharge contribute to summer hypoxia in the Changjiang (Yangtze) River Estuary?. *Science of the Total Environment*, 719: 137450, doi: [10.1016/j.scitotenv.2020.137450](#)
- Hao Qiang, Chai Fei, Xiu Peng, et al. 2019. Spatial and temporal variation in chlorophyll *a* concentration in the Eastern China Seas based on a locally modified satellite dataset. *Estuarine, Coastal and Shelf Science*, 220: 220–231, doi: [10.1016/j.ecss.2019.01.004](#)
- Karim R, Sekine M, Ukita M. 2003. A model of fish preference and mortality under hypoxic water in the coastal environment. *Marine Pollution Bulletin*, 47(1–6): 25–29, doi: [10.1016/S0025-326X\(02\)00409-5](#)

- Li Hongliang, Chen Jianfang, Lu Yong, et al. 2011. Seasonal variation of DO and formation mechanism of bottom water hypoxia of Changjiang River Estuary. *Journal of Marine Sciences (in Chinese)*, 29(3): 78–87, doi: [10.3969/j.issn.1001-909X.2011.03.010](https://doi.org/10.3969/j.issn.1001-909X.2011.03.010)
- Li Weiqi, Ge Jianzhong, Ding Pingxing, et al. 2021. Effects of dual fronts on the spatial pattern of chlorophyll-*a* concentrations in and off the Changjiang River estuary. *Estuaries and Coasts*, 44(5): 1408–1418, doi: [10.1007/s12237-020-00893-z](https://doi.org/10.1007/s12237-020-00893-z)
- Li Daoji, Zhang Jing, Huang Daji, et al. 2002. Oxygen depletion off the Changjiang (Yangtze River) Estuary. *Science in China Series D: Earth Sciences*, 45(12): 1137–1146, doi: [10.1360/02yd9110](https://doi.org/10.1360/02yd9110)
- Lie H J, Cho C H, Lee J H, et al. 2000. Seasonal variation of the Cheju Warm Current in the Northern East China Sea. *Journal of Oceanography*, 56(2): 197–211, doi: [10.1023/A:1011139313988](https://doi.org/10.1023/A:1011139313988)
- Lu Wenhai, Xiang Xianquan, Yang Lu, et al. 2017. The temporal-spatial distribution and changes of dissolved oxygen in the Changjiang Estuary and its adjacent waters for the last 50 a. *Acta Oceanologica Sinica*, 36(5): 90–98, doi: [10.1007/s13131-017-1063-6](https://doi.org/10.1007/s13131-017-1063-6)
- Luo Xiaofan, Wei Hao, Fan Renfu, et al. 2018. On influencing factors of hypoxia in waters adjacent to the Changjiang estuary. *Continental Shelf Research*, 152: 1–13, doi: [10.1016/j.csr.2017.10.004](https://doi.org/10.1016/j.csr.2017.10.004)
- Ma Xiao, Liu Anqi, Zhao Qiang, et al. 2022. Temporal variation of summer hypoxia off Changjiang estuary during 1997–2014 and its association with ENSO. *Frontiers in Marine Science*, 9: 897063, doi: [10.3389/fmars.2022.897063](https://doi.org/10.3389/fmars.2022.897063)
- Mann H B. 1945. Nonparametric tests against trend. *Econometrica*, 13(3): 245, doi: [10.2307/1907187](https://doi.org/10.2307/1907187)
- Meng Qicheng, Zhang Wenyan, Zhou Feng, et al. 2022. Water oxygen consumption rather than sediment oxygen consumption drives the variation of hypoxia on the East China Sea shelf. *Journal of Geophysical Research: Biogeosciences*, 127(2): e2021JG006705, doi: [10.1029/2021JG006705](https://doi.org/10.1029/2021JG006705)
- Ni Xiaobo, Huang Daji, Zeng Dingyong, et al. 2016. The impact of wind mixing on the variation of bottom dissolved oxygen off the Changjiang Estuary during summer. *Journal of Marine Systems*, 154: 122–130, doi: [10.1016/j.jmarsys.2014.11.010](https://doi.org/10.1016/j.jmarsys.2014.11.010)
- Ning Xiuren, Lin Chun, Su Jilan, et al. 2011. Long-term changes of dissolved oxygen, hypoxia, and the responses of the ecosystems in the East China Sea from 1975 to 1995. *Journal of Oceanography*, 67(1): 59–75, doi: [10.1007/s10872-011-0006-7](https://doi.org/10.1007/s10872-011-0006-7)
- Obenour D R, Michalak A M, Zhou Yuntao, et al. 2012. Quantifying the impacts of stratification and nutrient loading on hypoxia in the Northern Gulf of Mexico. *Environmental Science & Technology*, 46(10): 5489–5496, doi: [10.1021/es204481a](https://doi.org/10.1021/es204481a)
- Paerl H W. 2006. Assessing and managing nutrient-enhanced eutrophication in estuarine and coastal waters: interactive effects of human and climatic perturbations. *Ecological Engineering*, 26(1): 40–54, doi: [10.1016/j.ecoleng.2005.09.006](https://doi.org/10.1016/j.ecoleng.2005.09.006)
- Paerl H W, Pinckney J L, Fear J M, et al. 1998. Ecosystem responses to internal and watershed organic matter loading: consequences for hypoxia in the eutrophying Neuse River Estuary, North Carolina, USA. *Marine Ecology Progress Series*, 166: 17–25, doi: [10.3354/meps166017](https://doi.org/10.3354/meps166017)
- Park S, Chu P C, Lee J H. 2011. Interannual-to-interdecadal variability of the Yellow Sea Cold Water Mass in 1967–2008: characteristics and seasonal forcings. *Journal of Marine Systems*, 87(3–4): 177–193, doi: [10.1016/j.jmarsys.2011.03.012](https://doi.org/10.1016/j.jmarsys.2011.03.012)
- Qi Jifeng. 2014. The study on the water masses, Kuroshio and water exchange in the East China Sea (in Chinese)[dissertation]. Qingdao: Institute of Oceanology, Chinese Academy of Sciences
- Qian Wei, Dai Minhan, Xu Min, et al. 2017. Non-local drivers of the summer hypoxia in the East China Sea off the Changjiang Estuary. *Estuarine, Coastal and Shelf Science*, 198: 393–399, doi: [10.1016/j.ecss.2016.08.032](https://doi.org/10.1016/j.ecss.2016.08.032)
- Rabotyagov S S, Kling C L, Gassman P W, et al. 2014. The economics of dead zones: causes, impacts, policy challenges, and a model of the Gulf of Mexico hypoxic zone. *Review of Environmental Economics and Policy*, 8(1): 58–79, doi: [10.1093/reep/ret024](https://doi.org/10.1093/reep/ret024)
- Renaud M L. 1986. Hypoxia in Louisiana coastal waters during 1983: implications for fisheries. *Fishery Bulletin*, 84(1): 19–26
- Sen P K. 1968. Estimates of the regression coefficient based on Kendall's tau. *Journal of the American Statistical Association*, 63(324): 1379–1389, doi: [10.1080/01621459.1968.10480934](https://doi.org/10.1080/01621459.1968.10480934)
- Su Jilan, Huang Daji. 1995. On the current field associated with the Yellow Sea Cold Water Mass. *Oceanologia et Limnologia Sinica (in Chinese)*, 26(S5): 1–7
- Su Yusong, Li Fengqi, Wang Fengqin. 1996. Water distribution and water division in the Bohai Sea, Yellow Sea and East China Sea. *Haiyang Xuebao (in Chinese)*, 18(6): 1–7
- Sun Xiangdong, Liu Yongjun, Chen Wenwen, et al. 2010. Application of boxplot method in the validation of abnormal value of animal health data. *China Animal Health Inspection (in Chinese)*, 27(7): 66–68
- Theil H. 1992. A rank-invariant method of linear and polynomial regression analysis. In: Raj B, Koerts J, eds. *Henri Theil's Contributions to Economics and Econometrics*. Dordrecht: Springer
- Tian Di, Zhou Feng, Zhang Wenyan, et al. 2022. Effects of dissolved oxygen and nutrients from the Kuroshio on hypoxia off the Changjiang River estuary. *Journal of Oceanology and Limnology*, 40(2): 515–529, doi: [10.1007/s00343-021-0440-3](https://doi.org/10.1007/s00343-021-0440-3)
- Vaquer-Sunyer R, Duarte C M. 2008. Thresholds of hypoxia for marine biodiversity. *Proceedings of the National Academy of Sciences of the United States of America*, 105(40): 15452–15457, doi: [10.1073/pnas.0803833105](https://doi.org/10.1073/pnas.0803833105)
- Wan Yuming, Mei Xiuning, Zhou Yuhua. 1999. The medium-range process analysis of the flood disasters in the Yangtze River Basin in 1998 flood season. *Meteorological Monthly (in Chinese)*, 25(9): 24–30
- Wang Baodong. 2009. Hydromorphological mechanisms leading to hypoxia off the Changjiang estuary. *Marine Environmental Research*, 67(1): 53–58, doi: [10.1016/j.marenvres.2008.11.001](https://doi.org/10.1016/j.marenvres.2008.11.001)
- Wang Jiangtao, Cao Jing. 2012. Variation and effect of nutrient on phytoplankton community in Changjiang Estuary during last 50 years. *Marine Environmental Science*, 31(3): 310–315, doi: [10.3969/j.issn.1007-6336.2012.03.002](https://doi.org/10.3969/j.issn.1007-6336.2012.03.002)
- Wang Bin, Chen Jianfang, Jin Haiyan, et al. 2023. Subsurface oxygen minima regulated by remineralization and bottom flushing along 123°E in the inner East China Sea. *Frontiers in Marine Science*, 9: 1081975, doi: [10.3389/fmars.2022.1081975](https://doi.org/10.3389/fmars.2022.1081975)
- Wang Dianlai, Liu Wenping, Huang Xinyuan. 2013. Trend analysis in vegetation cover in Beijing based on Sen+Mann-Kendall method. *Computer Engineering and Applications (in Chinese)*, 49(5): 13–17, doi: [10.3778/j.issn.1002-8331.1206-0282](https://doi.org/10.3778/j.issn.1002-8331.1206-0282)
- Wang Dianlai, Su Aixia. 2019. Analysis of student's score based on box plot. *China Educational Technology & Equipment (in Chinese)*, (6): 98–99,106, doi: [10.3969/j.issn.1671-489X.2019.06.098](https://doi.org/10.3969/j.issn.1671-489X.2019.06.098)
- Wang Baodong, Wei Qinsheng, Chen Jianfang, et al. 2012. Annual cycle of hypoxia off the Changjiang (Yangtze River) Estuary. *Marine Environmental Research*, 77: 1–5, doi: [10.1016/j.marenvres.2011.12.007](https://doi.org/10.1016/j.marenvres.2011.12.007)
- Wang Wentao, Yu Zhiming, Song Xiuxian, et al. 2022. Hypoxia formation in the East China Sea by decomposed organic matter in the Kuroshio Subsurface Water. *Marine Pollution Bulletin*, 177: 113486, doi: [10.1016/J.MARPOLBUL.2022.113486](https://doi.org/10.1016/J.MARPOLBUL.2022.113486)
- Wang Yawei, Zhai Panmao, Tian Hua. 2006. Extreme high temperatures in southern China in 2003 under the background of climate change. *Meteorological Monthly (in Chinese)*, 32(10): 27–33, doi: [10.3969/j.issn.1000-0526.2006.10.004](https://doi.org/10.3969/j.issn.1000-0526.2006.10.004)
- Wei Hao, He Yunchang, Li Qingli, et al. 2007. Summer hypoxia adjacent to the Changjiang Estuary. *Journal of Marine Systems*, 67(3–4): 292–303, doi: [10.1016/j.jmarsys.2006.04.014](https://doi.org/10.1016/j.jmarsys.2006.04.014)
- Wei Qinsheng, Wang Baodong, Chen Jianfang, et al. 2015. Recognition on the forming-vanishing process and underlying mechanisms of the hypoxia off the Yangtze River estuary. *Science China: Earth Sciences*, 58(4): 628–648, doi: [10.1007/s11430-014-5007-0](https://doi.org/10.1007/s11430-014-5007-0)
- Wei Qinsheng, Wang Baodong, Zhang Xuelei, et al. 2021a. Contribu-

- tion of the offshore detached Changjiang (Yangtze River) Diluted Water to the formation of hypoxia in summer. *Science of the Total Environment*, 764: 142838, doi: [10.1016/j.scitotenv.2020.142838](https://doi.org/10.1016/j.scitotenv.2020.142838)
- Wei Qingsheng, Yao Qingzhen, Wang Baodong, et al. 2019. Deoxygenation and its controls in a semienclosed shelf ecosystem, Northern Yellow Sea. *Journal of Geophysical Research: Oceans*, 124(12): 9004–9019, doi: [10.1029/2019JC015399](https://doi.org/10.1029/2019JC015399)
- Wei Qingsheng, Yao Peng, Xu Bochao, et al. 2021b. Coastal upwelling combined with the river plume regulates hypoxia in the Changjiang estuary and adjacent inner East China Sea shelf. *Journal of Geophysical Research: Oceans*, 126(11): e2021JC017740, doi: [10.1029/2021JC017740](https://doi.org/10.1029/2021JC017740)
- Wishner K F, Seibel B A, Roman C, et al. 2018. Ocean deoxygenation and zooplankton: very small oxygen differences matter. *Science Advances*, 4(12): eaau5180, doi: [10.1126/sciadv.aau5180](https://doi.org/10.1126/sciadv.aau5180)
- Wu Hui, Zhu Jianrong, Shen Jian, et al. 2011. Tidal modulation on the Changjiang River plume in summer. *Journal of Geophysical Research: Oceans*, 116(C8): C08017, doi: [10.1029/2011JC007209](https://doi.org/10.1029/2011JC007209)
- Xuan Jiliang, Huang Daji, Zhou Feng, et al. 2012. The role of wind on the detachment of low salinity water in the Changjiang Estuary in summer. *Journal of Geophysical Research: Oceans*, 117(C10): C10004, doi: [10.1029/2012JC008121](https://doi.org/10.1029/2012JC008121)
- Yin Kedong, Lin Zhifeng, Ke Zhiyuan. 2004. Temporal and spatial distribution of dissolved oxygen in the Pearl River Estuary and adjacent coastal waters. *Continental Shelf Research*, 24(16): 1935–1948, doi: [10.1016/j.csr.2004.06.017](https://doi.org/10.1016/j.csr.2004.06.017)
- Zhang Haiyan, Fennel K, Laurent A, et al. 2020. A numerical model study of the main factors contributing to hypoxia and its interannual and short-term variability in the East China Sea. *Biogeosciences*, 17(22): 5745–5761, doi: [10.5194/bg-17-5745-2020](https://doi.org/10.5194/bg-17-5745-2020)
- Zhang J, Liu S, Ren J, et al. 2007. Nutrient gradients from the eutrophic Changjiang (Yangtze River) Estuary to the oligotrophic Kuroshio waters and re-evaluation of budgets for the East China Sea Shelf. *Progress in Oceanography*, 74(4): 449–478, doi: [10.1016/j.pocean.2007.04.019](https://doi.org/10.1016/j.pocean.2007.04.019)
- Zhang Wenxia, Moriarty J M, Wu Hui, et al. 2021. Response of bottom hypoxia off the Changjiang River Estuary to multiple factors: a numerical study. *Ocean Modelling*, 159: 101751, doi: [10.1016/j.ocemod.2021.101751](https://doi.org/10.1016/j.ocemod.2021.101751)
- Zhang S, Wang Q, Lü Y, et al. 2008. Observation of the seasonal evolution of the Yellow Sea Cold Water Mass in 1996–1998. *Continental Shelf Research*, 28(3): 442–457, doi: [10.1016/j.csr.2007.10.002](https://doi.org/10.1016/j.csr.2007.10.002)
- Zhang Wenxia, Wu Hui, Hetland R D, et al. 2019. On mechanisms controlling the seasonal hypoxia hot spots off the Changjiang River estuary. *Journal of Geophysical Research: Oceans*, 124(12): 8683–8700, doi: [10.1029/2019jc015322](https://doi.org/10.1029/2019jc015322)
- Zhang Jing, Xiao Tian, Huang Daji, et al. 2016. Editorial: Eutrophication and hypoxia and their impacts on the ecosystem of the Changjiang Estuary and adjacent coastal environment. *Journal of Marine Systems*, 154: 1–4, doi: [10.1016/j.jmarsys.2015.10.007](https://doi.org/10.1016/j.jmarsys.2015.10.007)
- Zhao Qiang, Cai Yanhong, He Shanfang, et al. 2015. Optimal interpolation assimilation experiments based on the data from section investigation in the East China Sea. *Marine Science Bulletin (in Chinese)*, 34(3): 275–282, doi: [10.11840/j.issn.1001-6392.2015.03.006](https://doi.org/10.11840/j.issn.1001-6392.2015.03.006)
- Zhao Huade, Kao Shuhji, Zhai Weidong, et al. 2017. Effects of stratification, organic matter remineralization and bathymetry on summertime oxygen distribution in the Bohai Sea, China. *Continental Shelf Research*, 134: 15–25, doi: [10.1016/j.csr.2016.12.004](https://doi.org/10.1016/j.csr.2016.12.004)
- Zhou Feng, Chai Fei, Huang Daji, et al. 2017. Investigation of hypoxia off the Changjiang Estuary using a coupled model of ROMS-CoSiNE. *Progress in Oceanography*, 159: 237–254, doi: [10.1016/j.pocean.2017.10.008](https://doi.org/10.1016/j.pocean.2017.10.008)
- Zhou Feng, Chai Fei, Huang Daji, et al. 2020. Coupling and decoupling of high biomass phytoplankton production and hypoxia in a highly dynamic coastal system: the Changjiang (Yangtze River) estuary. *Frontiers in Marine Science*, 7: 259, doi: [10.3389/fmars.2020.00259](https://doi.org/10.3389/fmars.2020.00259)
- Zhou Feng, Huang Daji, Ni Xiaobo, et al. 2010. Hydrographic analysis on the multi-time scale variability of hypoxia adjacent to the Changjiang River Estuary. *Acta Ecologica Sinica (in Chinese)*, 30(17): 4728–47407
- Zhou Feng, Qian Zhouyi, Liu Anqi, et al. 2021a. Recent progress on the studies of the physical mechanisms of hypoxia off the Changjiang (Yangtze River) Estuary. *Journal of Marine Sciences (in Chinese)*, 39(4): 22–38, doi: [10.3969/j.issn.1001-909X.2021.04.003](https://doi.org/10.3969/j.issn.1001-909X.2021.04.003)
- Zhou Mingjiang, Shen Zhiliang, Yu Rencheng. 2008. Responses of a coastal phytoplankton community to increased nutrient input from the Changjiang (Yangtze) River. *Continental Shelf Research*, 28(12): 1483–1489, doi: [10.1016/j.csr.2007.02.009](https://doi.org/10.1016/j.csr.2007.02.009)
- Zhou Feng, Xuan Jiliang, Ni Xiaobo, et al. 2009. A preliminary study on variations of the Changjiang Diluted Water between August 1999 and 2006. *Acta Oceanologica Sinica*, 28(6): 1–11
- Zhou Jun, Zhu Zhuoyi, Hu Huanting, et al. 2021b. Clarifying water column respiration and sedimentary oxygen respiration under oxygen depletion off the Changjiang estuary and adjacent East China Sea. *Frontiers in Marine Science*, 7: 623581, doi: [10.3389/fmars.2020.623581](https://doi.org/10.3389/fmars.2020.623581)
- Zhu Zhuoyi, Wu Hui, Liu Sumei, et al. 2017. Hypoxia off the Changjiang (Yangtze River) estuary and in the adjacent East China Sea: quantitative approaches to estimating the tidal impact and nutrient regeneration. *Marine Pollution Bulletin*, 125(1–2): 103–114, doi: [10.1016/j.marpolbul.2017.07.029](https://doi.org/10.1016/j.marpolbul.2017.07.029)
- Zhu Zhuoyi, Zhang Jing, Wu Ying, et al. 2011. Hypoxia off the Changjiang (Yangtze River) Estuary: oxygen depletion and organic matter decomposition. *Marine Chemistry*, 125(1–4): 108–116, doi: [10.1016/j.marchem.2011.03.005](https://doi.org/10.1016/j.marchem.2011.03.005)
- Zhu Jianrong, Zhu Zhuoyi, Lin Jun, et al. 2016. Distribution of hypoxia and pycnocline off the Changjiang Estuary, China. *Journal of Marine Systems*, 154: 28–40, doi: [10.1016/j.jmarsys.2015.05.002](https://doi.org/10.1016/j.jmarsys.2015.05.002)
- Zou Emei, Guo Binghuo, Tang Yuxiang, et al. 2001. An analysis of summer hydrographic features and circulation in the southern Yellow Sea and the northern East China Sea. *Oceanologia et Limnologia Sinica (in Chinese)*, 32(3): 340–347, doi: [10.3321/j.issn:0029-814X.2001.03.016](https://doi.org/10.3321/j.issn:0029-814X.2001.03.016)

Supplementary information:

Fig. S1. Distribution of DO concentration along the Jeju-do Island section.

Fig. S2. Temperature-salinity diagrams of Section S1 (blue and green dots) compared with those of climatology [gray dot, based on Chen (1992)].

Table S1. Sampling depth and location along Section S1.

Table S2. Trends in dissolved oxygen (DO), apparent oxygen utilization (AOU), temperature (T), salinity (S), nitrate concentration, phosphate concentration, minimum dissolved oxygen (DO_{\min}), thickness of hypoxia (H), stratification ($d\rho$) and primary productivity (Area) at each depth range.

The supplementary information is available online at <https://doi.org/10.1007/s13131-023-2244-0> and <http://www.aosocean.com/>. The supplementary information is published as submitted, without typesetting or editing. The responsibility for scientific accuracy and content remains entirely with the authors.